

Crystal field effects in RCu_2Si_2 compounds ($\text{R} = \text{Ce}, \text{Pr}, \text{Nd}, \text{Ho}, \text{Er}$): Inelastic neutron scattering investigation

E. A. Goremychkin and A. Yu. Muzychka

Joint Institute of Nuclear Research, 141980 Dubna, Moscow District, Russia

R. Osborn

Materials Science Division, Argonne National Laboratory, Argonne, Illinois 60439-4845 USA

(Submitted 13 May 1995; resubmitted 4 April 1996)

Zh. Éksp. Teor. Fiz. **110**, 1339–1354 (October 1996)

The crystal field parameters in the family of isostructural RCu_2Si_2 compounds ($\text{R} = \text{Ce}, \text{Pr}, \text{Nd}, \text{Ho}, \text{Er}$) have been determined by the method of inelastic magnetic neutron scattering.

Comparative analysis of the parameters on the basis of the superposition model of the crystal field showed that the hybridization of the f electrons of cerium and the p electrons of silicon is the dominant component of the crystal field in the heavy-fermion compound CeCu_2Si_2 and it is responsible for the anomalous electronic properties of this compound. Analysis of the macroscopic properties of PrCu_2Si_2 based on the parameters determined in the present work for the crystal field split ground-state multiplet of the Pr^{+3} ion showed that their behavior can be interpreted as crystal-field effects and not a manifestation of anomalous electronic properties (quadrupole Kondo effect). © 1996 American Institute of Physics. [S1063-7761(96)01410-2]

1. INTRODUCTION

The magnetic, transport, thermodynamic, and other properties of compounds of rare-earth (RE) metals are largely determined by the interaction of the $4f$ -electron shell with the crystal field. Therefore a key aspect in investigations in the physics of compounds of RE metals is the knowledge and understanding of the characteristics of this interaction.

Two basic components, which determine the magnitude of the crystal field potential, can be identified in metal compounds: the contribution of the ion cores (ligands) and the contribution of conduction electrons. At present it is impossible to estimate these contributions on the basis of a microscopic model of the crystal field, and a phenomenological model of the crystal field is essentially the only method available for analyzing the properties of compounds containing RE metals. In this model the parameters of the crystal field potential are determined by comparing the computed and experimentally determined properties of the RE-metal compounds of interest. Despite the large number of experimental works on the crystal field, it has not yet been possible to establish with adequate reliability the principles involved in the formation of the crystal field potential in RE-metal compounds.¹ One reason for this is the lack of estimates of the magnitudes of the individual components of the crystal field potential in metallic systems.

Another important circumstance in the study of crystal-field effects in RE-metal compounds is the role of these effects in the physics of systems with an anomalous $s-f$ interaction (systems with heavy fermions, intermediate valence, and so on). For example, theoretical estimates show that $s-f$ hybridization, which is responsible for the anomalous properties of compounds with heavy fermions, makes the main contribution to the crystal field potential.² This as-

sertion can be checked experimentally by means of a systematic investigation of the crystal field in both normal and anomalous RE-metal compounds.

One of the most interesting families of isostructural intermetallic compounds is RM_2X_2 compounds (R —RE metal, M —transition metal, $\text{X} = \text{Ge}, \text{Si}$) with ThCr_2Si_2 type structure.³ This family of compounds incorporates a very diverse types of basic compounds. For example, CeCu_2Si_2 is a heavy-fermion superconducting compound, CeM_2Si_2 ($\text{M} = \text{Ni}, \text{Co}, \text{Fe}$) are intermediate-valence systems, and at low temperatures CeCu_2Ge_2 is a Kondo system with an antiferromagnetic order. At low temperatures RNi_2Si_2 compounds ($\text{R} = \text{Pr}, \text{Nd}, \text{Tb}, \text{Ho}, \text{Er}, \text{Tm}$) possess nontrivial magnetic structures which are incommensurate with the atomic structure.^{3,4} Therefore, one can attempt to establish a correlation between the characteristics of the crystal field and the type of ground state by investigating the crystal field of the isostructural RM_2X_2 compounds. To this end, we started systematic investigations of crystal field effects in RM_2X_2 compounds. In the present paper we report the results of a study of RCu_2Si_2 compounds ($\text{R} = \text{Ce}, \text{Pr}, \text{Nd}, \text{Ho}, \text{Er}$). In Refs. 5–7 we published some results of a study of compounds in this series.

Among the different methods for studying the crystal field in RE-metal compounds, inelastic scattering of thermal neutrons is special. The scattering law $S(Q, \omega)$ measured in experiments on the inelastic scattering of thermal neutrons is most closely related to the parameters of the split ground-state multiplet of the RE-metal ion in the experimental system. For example, the positions of the peaks in $S(Q, \omega)$ will correspond to the energy splitting between the levels of the crystal-field split ground-state multiplet, and their intensity will be proportional to the mixing coefficients of the wave functions of these levels. Therefore, the inelastic scattering

of thermal neutrons, being a direct spectroscopic method, gives the most reliable information about the characteristics of the crystal field, and it was used in the present work to investigate the crystal field in RCu_2Si_2 compounds.

2. EXPERIMENT

Samples of RCu_2Si_2 compounds were prepared by arc melting on a copper water-cooled hearth with no weight loss during the melting process. After vacuum annealing at 700°C , x-ray crystallographic analysis and neutron diffraction experiments showed that there were no other phases in any samples, with the exception of samples with Pr and Nd, where weak diffraction peaks that do not belong to the main phase were observed. The amount of the extraneous phases in these samples was estimated to be $\sim 5\%$, which cannot affect the experimental results on the inelastic scattering of thermal neutrons.

The inelastic thermal-neutron scattering experiments were performed on two spectrometers: an HET time-of-flight spectrometer with direct geometry at the ISIS spallation neutron source (RAL, UK) and a KDSOG-M time-of-flight spectrometer with inverse geometry in a pulsed IBR-2 reactor (JINR, Russia). These two spectrometers with mutually complementary characteristics made it possible to increase substantially the reliability of the results obtained.⁵ For example, the wide range of transferred energies and the high intensity of the KDSOG-M spectrometer made it possible to record reliably the total splitting of the ground-state multiplet. This made it possible, in addition, to optimize the HET experiment performed with a higher resolution and low momentum transfer, which in turn made it possible to refine the crystal-field parameters by making a profile fit of the inelastic thermal-neutron scattering spectra.

The HET experiments were conducted at incident neutron energies of 15 and 25 meV with resolutions of 0.4 and 0.75 meV, respectively. A ~ 50 g sample in an aluminum container was mounted on a closed-cycle refrigerator, which made it possible to obtain temperatures from 10 to 300 K. A helium cryostat (Orange cryostat) was used for the inelastic thermal-neutron scattering measurements below 10 K. The spectra employed for analysis were measured at scattering angles from 10° to 30° and then summed. This corresponded to an average momentum transfer (Q) of $\sim 0.9 \text{ \AA}$ on the elastic line with an incident energy of 15 meV. Comparing the spectra for this angular range with the spectra obtained at a scattering angle of 136° ($Q = 5 \text{ \AA}$) showed that the phonon contribution is negligibly small for all experimental samples.

The experiments performed with the KDSOG-M spectrometer in inverse geometry were conducted with a large sample (~ 100 g), placed in an aluminum container in a helium-flow cryostat. The inelastic thermal-neutron scattering measurements were performed at temperatures of 10 and 77 K. Since the momentum transfer in the KDSOG-M experiments is larger than in the HET case, the phonon contribution becomes appreciable and an allowance must be made for it when analyzing the experimental data. For this, inelastic thermal-neutron scattering experiments were performed under the same conditions with the isostructural compound

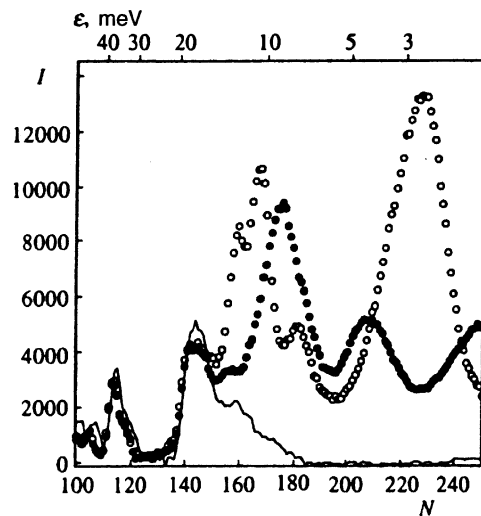


FIG. 1. PrCu_2Si_2 and LaCu_2Si_2 time-of-flight inelastic neutron scattering spectra obtained with the KDSOG-M spectrometer. The number of the time channel is plotted along the abscissa (the corresponding energy transfers are indicated at the top) and the neutron count is plotted along the ordinate. curve— LaCu_2Si_2 , $T = 80$ K; open circles— PrCu_2Si_2 , $T = 10$ K; filled circles— PrCu_2Si_2 , $T = 80$ K.

LaCu_2Si_2 , where magnetic scattering does not occur. It was found that for all experimental RCu_2Si_2 samples magnetic scattering occurs with energy transfers of less than 15 meV. As one can see from Fig. 1 (solid line), the phonon contribution is relatively small in this range of energy transfer, so that the possible systematic errors associated with the use of the LaCu_2Si_2 spectrum (corrected for the difference in the scattering amplitudes between La and other RE metals) to estimate the phonon contribution should not greatly influence the results for the crystal-field parameters.

The experimental RCu_2Si_2 compounds are all antiferromagnetic at low temperatures ($T < 21$ K). The appearance of antiferromagnetic ordering has a strong effect on the spectrum of magnetic excitations (Fig. 1), and in interpreting these spectra, in addition to the crystal field, allowance must be made for the interaction between the $4f$ -magnetic moments of the RE-metal ions. In the present paper we shall discuss only the experimental results on the inelastic thermal-neutron scattering in the paramagnetic state.

3. ANALYSIS OF EXPERIMENTAL DATA

The scattering law for unpolarized neutrons in the dipole approximation has the form⁸

$$S(Q, \varepsilon, T) = F^2(Q) \exp(-2W) \frac{\varepsilon/kT}{1 - \exp(-\varepsilon/kT)} g_J^2 \times \sum_{ij} \rho_i |\langle j | J_\perp | i \rangle|^2 \frac{1 - \exp(-\Delta_{ij}/kT)}{\Delta_{ij}/kT} P(\varepsilon - \Delta_{ij}, \Gamma_{ij}), \quad (1)$$

where Q is the neutron momentum transfer, ε is the neutron energy transfer, T is the temperature, $F(Q)$ is the magnetic form factor, $\exp(-2W)$ is the Debye-Waller factor, g_J is the Landé factor, ρ_i is the occupancy of the level from which the transition occurs, Δ_{ij} is the energy difference between the

states $|i\rangle$ and $|j\rangle$, J_{\perp} is the component of the total angular momentum of the RE-metal ion that is perpendicular to the scattering vector \mathbf{Q} , and $P(\varepsilon, \Gamma)$ is the spectral function, normalized to unity.

In the experimental compounds the RE-metal ions occupy sites with tetragonal point symmetry. The crystal-field Hamiltonian for this symmetry has the form

$$H_{CF} = B_2^0 O_2^0 + B_4^0 O_4^0 + B_4^4 O_4^4 + B_6^0 O_6^0 + B_6^4 O_6^4, \quad (2)$$

where O_l^m are the equivalent Stevens operators⁹ and B_l^m are the phenomenological crystal-field parameters.

The expression for the squared matrix elements $\langle i|J_{\perp}|j\rangle$, which describes the relative intensity of the transitions between the crystal-field levels, has the form

$$|\langle i|J_{\perp}|j\rangle|^2 = \frac{1}{3} |\langle i|J_{-}|j\rangle|^2 + \frac{1}{3} |\langle i|J_{+}|j\rangle|^2 + \frac{2}{3} |\langle i|J_z|j\rangle|^2. \quad (3)$$

The crystal field parameters were determined from the inelastic thermal-neutron scattering spectra in two steps. First, the Hamiltonian was parameterized in the form¹⁰

$$H = W \left[(1 - |x_1| - |x_2| - |x_3| - |x_4|) \frac{O_2^0}{F_{20}} + \frac{x_1 O_4^0}{F_{40}} + \frac{x_2 O_4^4}{F_{44}} + \frac{x_3 O_6^0}{F_{60}} + \frac{x_4 O_6^4}{F_{64}} \right], \quad (4)$$

where F_{mn} are numerical factors taken from Ref. 10 and the parameters x_i are related with the parameters B_l^m by the following relations:

$$B_2^0 = \frac{W}{F_{20}} (1 - |x_1| - |x_2| - |x_3| - |x_4|), \quad B_4^0 = \frac{W x_1}{F_{40}},$$

$$B_4^4 = \frac{W x_2}{F_{44}}, \quad B_6^0 = \frac{W x_3}{F_{60}}, \quad B_6^4 = \frac{W x_4}{F_{64}}.$$

The convenience of this parameterization lies in the fact that the range of variation of the parameters x_i is limited by the condition

$$\sum_i |x_i| \leq 1,$$

and the parameter W is a scale factor determining the total splitting of the ground-state multiplet in a crystal field. It can be fixed for a given set of x_i , if it is possible to determine from the experimental data, for example, the total splitting in the crystal field or the sequence number of one of the excited levels relative to the ground state. The first step in searching for the crystal-field parameters with the Hamiltonian (4) was to scan the entire space of the parameters $\{x_i\}$ with a constant step in x_i . In the process, the parameter sets which could describe well the basic features of the inelastic thermal-neutron scattering spectra were selected.

At the second step the final determination of the crystal field parameters was made by making a least-squares fit of the computed spectra to the experimentally measured spectra

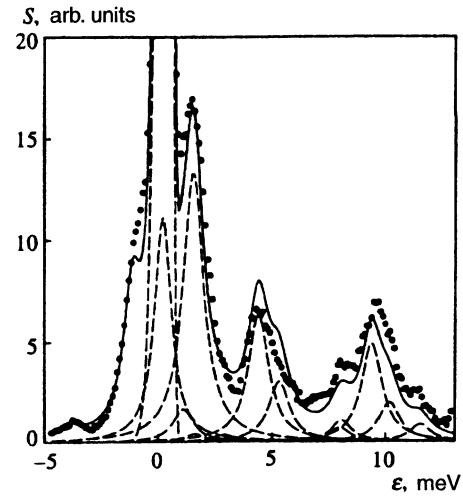


FIG. 2. Scattering law obtained with the HET spectrometer for PrCu_2Si_2 at $T=25$ K. Dots—experimental spectrum; solid line—computed spectrum, dashed lines—separate spectral components.

taking account of the resolution function. In the process, it was assumed that all transitions have the same widths and a Lorentzian distribution, which described the profile of the transitions between the crystal-field levels much better than a Gaussian distribution.

4. EXPERIMENTAL RESULTS

4.1. PrCu_2Si_2

The ground-state multiplet 3H_4 of the Pr^{+3} ion in a tetragonal crystal field splits into seven levels: two doublets and five singlets. The experimental results on the inelastic thermal-neutron scattering are presented in Figs. 1, 2, and 3. As one can see from these figures, in the paramagnetic state ($T_N=21$ K) there are three groups of peaks of magnetic

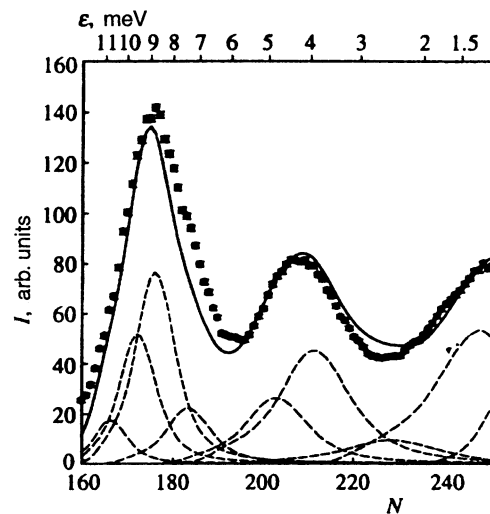


FIG. 3. PrCu_2Si_2 time-of-flight inelastic magnetic neutron scattering spectrum obtained with the KDSOG-M spectrometer at $T=80$ K. The number of the time channel is plotted along the abscissa (the corresponding energy transfers are indicated at the top). Dots—experimental spectrum, solid line—computed spectrum, dashed lines—separate spectral components.

TABLE I. Crystal field parameters of CeCu_2Si_2 and the compounds investigated. $A_l^m(r^l)$ equal the parameters B_l^m divided by the corresponding Stevens factors; these are the crystal-field parameters which are freed, to the greatest extent possible, from the peculiarities corresponding to RE metals.

P3	B_2^0 , meV $A_2^0(r^2)$, meV	B_4^0 , meV $A_4^0(r^4)$, meV	B_4^4 , meV $A_4^4(r^4)$, meV	B_6^0 , meV $A_6^0(r^6)$, meV	B_6^4 , meV $A_6^4(r^6)$, meV
Ce	-1.29 ± 0.01 22.59	$-(4.34 \pm 0.03) \cdot 10^{-3}$ -0.68	$\pm 0.453 \pm 0.003$ ± 71.34		
Pr	-0.063 ± 0.005 3.00	$(1.48 \pm 0.10) \cdot 10^{-3}$ -2.01	$\mp (2.24 \pm 0.05) \cdot 10^{-2}$ ± 30.56	$(5.27 \pm 0.30) \cdot 10^{-5}$ 0.86	$\pm (3.80 \pm 0.05) \cdot 10^{-4}$ ± 6.23
Nd	-0.031 ± 0.001 4.82	$(1.10 \pm 0.10) \cdot 10^{-3}$ -3.94	$\mp (1.33 \pm 0.04) \cdot 10^{-3}$ ± 4.77	$-(3.17 \pm 0.04) \cdot 10^{-5}$ 0.87	$\mp (6.62 \pm 0.02) \cdot 10^{-4}$ ± 18.19
Ho	0.028 ± 0.003 -12.58	$(8.60 \pm 0.05) \cdot 10^{-5}$ -2.58	$\mp (1.33 \pm 0.03) \cdot 10^{-4}$ ± 4.00	$-(4.50 \pm 0.10) \cdot 10^{-7}$ 0.34	$\mp (1.62 \pm 0.04) \cdot 10^{-5}$ ± 12.43
Er	-0.160 ± 0.002 -6.20	$-(1.27 \pm 0.08) \cdot 10^{-4}$ -2.68	$\mp (3.00 \pm 0.15) \cdot 10^{-4}$ ± 6.30	$(5.00 \pm 0.40) \cdot 10^{-7}$ 0.30	$\pm (2.90 \pm 0.10) \cdot 10^{-5}$ ± 13.56

origin with energy transfers of 1.5, 4.3, and 9.2 meV. A set of parameters best describing the experimentally measured spectra was determined using the search procedure described above for the crystal field parameters. The values of the parameters are given in Table I. The corresponding scheme of the levels and their wave functions are presented in Fig. 4. On the whole, as one can see from Fig. 2 and 3, the agreement between the computed and experimental spectra is not bad. The small discrepancies could be due to the fact that the width was assumed to be the same for all transitions and to the fact that PrCu_2Si_2 has an anomalously high temperature T_N , and for this reason the energy of transitions in a crystal field can exhibit a weak dispersion. A more detailed discussion of the inelastic thermal-neutron scattering data for PrCu_2Si_2 is given in Ref. 7.

4.2. NdCu_2Si_2

A tetragonal crystal field splits the ground-state multiplet $^4I_{9/2}$ of the Nd^{+3} ion into five Kramers doublets. NdCu_2Si_2 was the first compound from the family of intermetallic com-

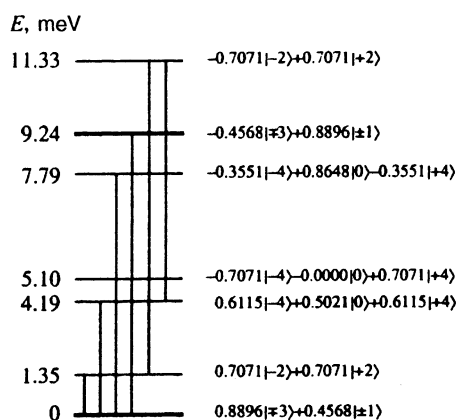


FIG. 4. Level scheme and structure of the wave functions corresponding to the splitting of the ground-state multiplet of Pr in the crystal field of PrCu_2Si_2 . The vertical lines represent the experimentally observed dipole transitions.

pounds RM_2X_2 where the crystal field parameters were determined by the method of inelastic thermal-neutron scattering. The main HET results for this system were published in Ref. 6. Figure 5 displays the inelastic thermal-neutron scattering spectra (dots) measured at 77 K with the KDSOG-M spectrometer. Just as in the case of the HET experiments,⁶ there is good agreement between the computed spectra (solid line in Fig. 5) and the experimental spectra. The crystal field parameters for NdCu_2Si_2 are given in Table I, and the corresponding level scheme is displayed in Fig. 6.

4.3 HoCu_2Si_2

The ground-state multiplet 5I_8 of the Ho^{+3} ion in a tetragonal field splits into four doublets and nine singlets with a large number of possible transitions from both the ground and excited states. Figure 7 displays the spectrum of HoCu_2Si_2 in the paramagnetic state ($T_N = 10$ K). The spec-

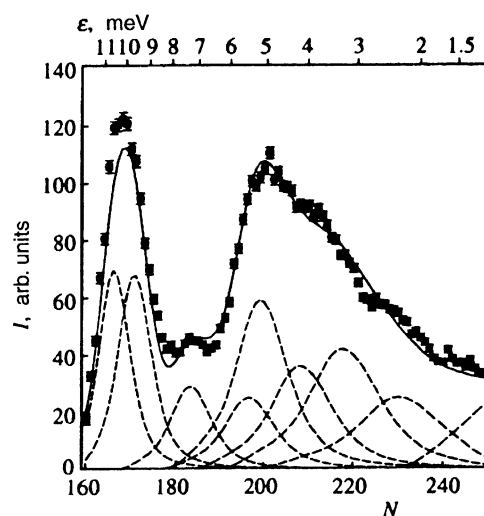


FIG. 5. NdCu_2Si_2 time-of-flight inelastic magnetic scattering spectrum obtained with a KDSOG-M spectrometer at $T = 80$ K. The number of the time channel is plotted along the abscissa (the corresponding energy transfers are indicated at the top). Dots—experimental spectrum, solid line—computed spectrum, dashed lines—separate spectral components.

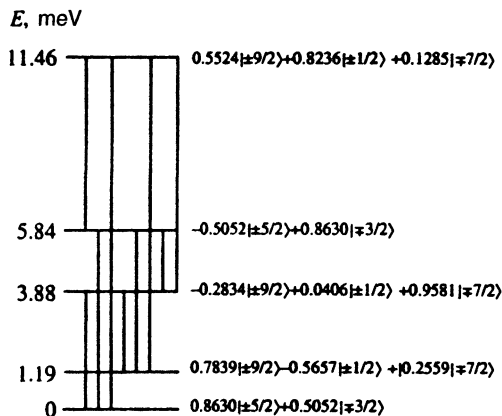


FIG. 6. Level scheme and structure of the wave functions corresponding to the splitting of the ground-state multiplet of Nd in the crystal field of NdCu_2Si_2 . The vertical lines represent the experimentally observed dipole transitions.

trum was measured on the HET spectrometer with $E_0 = 15$ meV and $T = 15$ K. As one can see in this figure, there are four regions where inelastic magnetic scattering associated with crystal-field transitions occurs: $\varepsilon < 2$ meV, $\varepsilon \sim 3$ meV, $4 \text{ meV} < \varepsilon < 7$ meV, and $7 \text{ meV} < \varepsilon < 10$ meV. The HET measurements with a lower initial energy (10 meV) and, correspondingly, better energy resolution did not make it possible to resolve separate transitions between crystal-field levels. This is due mainly to the large number of transitions from excited states lying at energies of less than 2 meV and having a substantial occupancy at $T = 15$ K. Nonetheless, we were able to obtain a reliable set of crystal-field parameters which satisfactorily describe the experimental spectra from both the HET spectrometer at 15 K (Fig. 7) and the KDSOG-M spectrometer at $T = 77$ K (Fig. 8). Their values are presented in Table I. The level scheme and the wave functions are presented in Fig. 9.

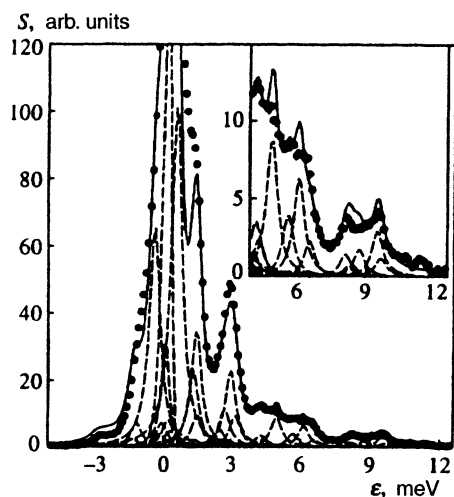


FIG. 7. Scattering law obtained with the HET spectrometer for HoCu_2Si_2 at $T = 15$ K. Dots—experimental spectrum, solid lines—computed spectrum, dashed lines—separate spectral components. Inset: Relatively weak part of the spectrum corresponding to the region of energy transfers exceeding 4 meV.

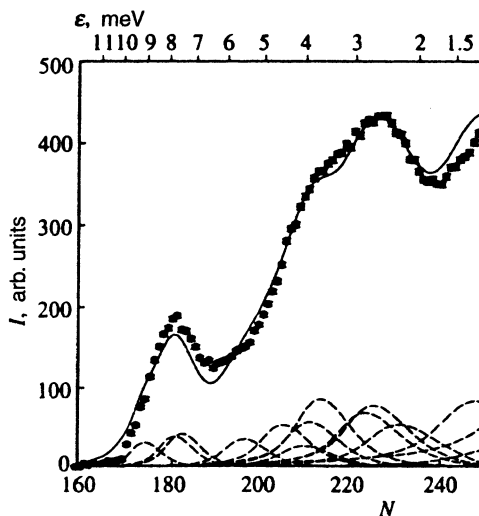


FIG. 8. HoCu_2Si_2 time-of-flight inelastic magnetic scattering spectrum obtained with a KDSOG-M spectrometer at $T = 80$ K. The number of the time channel is plotted along the abscissa (the corresponding energy transfers are indicated at the top). Dots—experimental spectrum, solid line—computed spectrum, dashed lines—separate spectral components.

4.4. ErCu_2Si_2

The ground-state multiplet $^4I_{15/2}$ of the Kramers ion Er^{+3} in a tetragonal field splits into eight doublets. On account of the low Néel temperature ($T_N < 2$ K), the inelastic thermal-neutron scattering experiments could be performed in the paramagnetic phase at low temperatures. The HET spectra measured at $E_0 = 15$ meV and $T = 4.5$ and 30 K and the KDSOG-M spectra measured at $T = 10$ and 77 K are presented in Figs. 10 and 11. Comparing the intensities of the peaks in the spectra at different temperatures gives unambiguously the position of seven of the eight levels of the crystal-field split ground-state multiplet of the Er^{+3} ion in

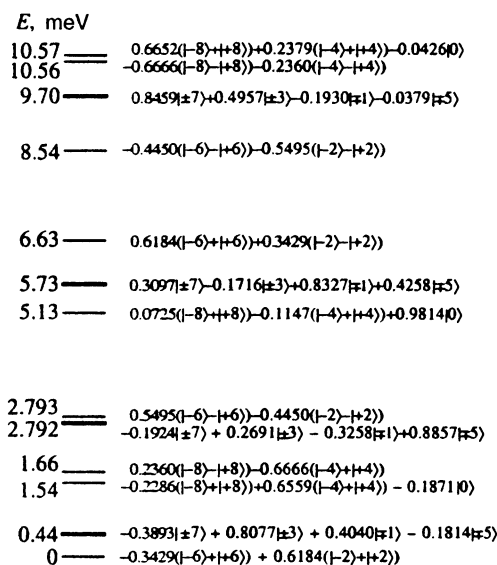


FIG. 9. Level scheme and structure of the wave functions corresponding to the splitting of the ground-state multiplet of Ho in the crystal field of HoCu_2Si_2 .

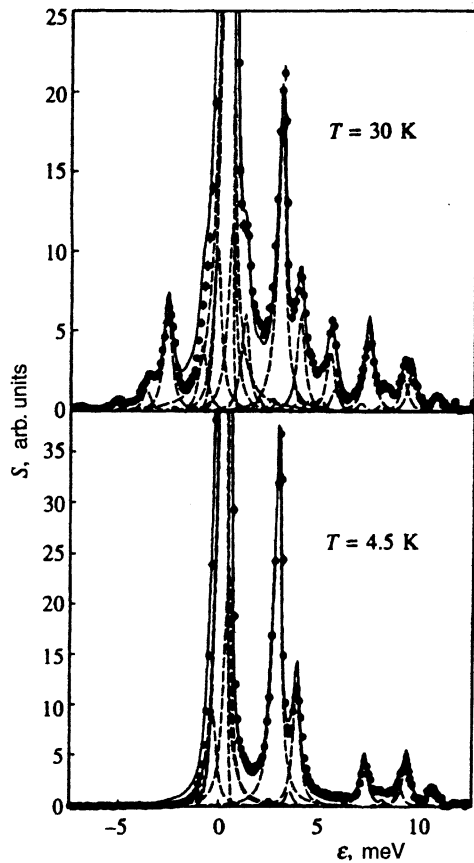


FIG. 10. Scattering law obtained with the HET spectrometer for ErCu_2Si_2 at different temperatures. Dots—experimental spectrum, solid lines—computed spectrum, dashed lines—separate spectral components.

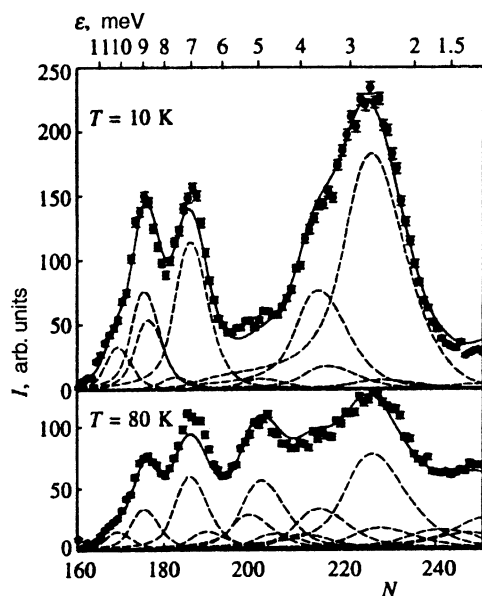


FIG. 11. ErCu_2Si_2 time-of-flight inelastic magnetic scattering spectrum obtained with a KDSOG-M spectrometer at different temperatures. The number of the time channel is plotted along the abscissa (the corresponding energy transfers are indicated at the top). Dots—experimental spectrum, solid line—computed spectrum, dashed lines—separate spectral components.

E , meV	
10.54	$-0.3349(\pm 1/2) - 0.4831(\pm 3/2) + 0.6841(\pm 5/2) + 0.4316(\pm 13/2)$
9.25	$0.4296(\pm 15/2) + 0.8690(\pm 7/2) - 0.2207(\pm 1/2) - 0.1073(\pm 9/2)$
7.91	$0.7179(\pm 1/2) + 0.4126(\pm 3/2) + 0.3869(\pm 5/2) + 0.4057(\pm 13/2)$
7.54	$0.0856(\pm 15/2) + 0.1320(\pm 7/2) + 0.2179(\pm 1/2) + 0.9632(\pm 9/2)$
3.78	$0.2315(\pm 15/2) + 0.1028(\pm 7/2) + 0.9399(\pm 1/2) - 0.2457(\pm 9/2)$
2.77	$-0.5724(\pm 1/2) + 0.6414(\pm 3/2) - 0.1376(\pm 5/2) + 0.4919(\pm 13/2)$
0.18	$0.8732(\pm 15/2) - 0.4657(\pm 7/2) - 0.1427(\pm 1/2) + 0.0185(\pm 9/2)$
0	$0.2114(\pm 1/2) - 0.4300(\pm 3/2) - 0.6028(\pm 5/2) + 0.6380(\pm 13/2)$

FIG. 12. Level scheme and structure of the wave functions corresponding to the splitting of the ground-state multiplet of Er in the crystal field of ErCu_2Si_2 .

ErCu_2Si_2 . Analysis of the inelastic thermal-neutron scattering data by the procedure described above made it possible to determine the set of crystal-field parameters which described well both the HET and the KDSOG-M spectra (solid lines in Fig. 10 and 11). The parameters of the crystal-field Hamiltonian for ErCu_2Si_2 are presented in Table I, and the corresponding level scheme and the wave functions are presented in Fig. 12

5. DISCUSSION

In the present section we present a comparative analysis of the results for the crystal-field parameters with the aim of clarifying the degree to which their values are correlated with the properties of the compounds studied. We shall devote special attention to the two systems CeCu_2Si_2 and PrCu_2Si_2 . These compounds are singled out from because of their anomalous electronic properties.

The compound CeCu_2Si_2 is a superconducting system with heavy fermions. In Ref. 5, analysis of the crystal-field parameters for this compound in a superposition model of the crystal field showed that the hybridization of the $4f$ -electronic states with the p orbitals of Si is the dominant component of the crystal field and it is apparently responsible for the anomalous electronic properties of this compound.

The compound PrCu_2Si_2 is an antiferromagnet ($T_N = 21$ K) with an anomalously high Néel temperature compared with GdCu_2Si_2 ($T_N = 13.5$ K). In Refs. 11–13, it is classified, on the basis of measurements of different macroscopic properties, as a heavy-fermion system.

The parameters $A_l^m \langle r^l \rangle$ without the Stevens factor, thereby making possible to compare the crystal-field parameters for different RE-metal ions, are given in Table I together with the parameters B_l^m . In analyzing the crystal-field parameters of compounds in which the RE-metal ion possesses tetragonal point symmetry, it should be kept in mind that it is impossible to determine unambiguously from inelastic thermal-neutron scattering experiments the signs of the parameters B_4^4 and B_6^4 in the Hamiltonian (2).

As one can see from Table I, the values of $A_l^m\langle r^l \rangle$ for CeCu_2Si_2 are substantially different from the corresponding values of $A_l^m\langle r^l \rangle$ for the other RCu_2Si_2 compounds. For example, $A_4^4\langle r^4 \rangle$ differs by approximately a factor of 14 from the values for the compounds containing Nd, Ho, and Er. Such a difference itself indicates the anomalous character of the crystal field potential in CeCu_2Si_2 . However, the crystal structure of the compounds RCu_2Si_2 has an interesting feature that makes it possible to employ the superposition model of the crystal field⁵ for quantitative estimation of the contributions of different ligands to the crystal-field potential and therefore to identify the component that makes it anomalous. This feature is that the RE-metal ion is surrounded by two almost equidistant coordination spheres consisting of eight silicon atoms and eight copper atoms. In the superposition model of the crystal field¹⁴ it is assumed that the crystal field can be represented as a superposition of the potentials of different coordination spheres. From the standpoint of the superposition model, the contribution of each coordination sphere to the value of the crystal-field parameter can be represented as the product of the geometric coordination factor \bar{K}_{lm} , which depends on the arrangement of the ions on a sphere, and the parameter $\tilde{A}_l(R_j)$, which will determine the contribution of the ions of a given coordination sphere to the crystal field:

$$B_l^m = \Theta_l \sum_{ij} \tilde{A}_l(R_j) K_{lm}(\theta_i, \phi_i). \quad (5)$$

Here, Θ_l is the Steven factor and R_j , θ_i , and ϕ_i are, respectively, the coordinates of the i th ion in the j th coordination sphere.

The possibility of neglecting the contributions to Eq. (5) from the distant coordination spheres was discussed in Ref. 14, and it was concluded that in the case of the fourth- and sixth-order crystal fields only the contribution of the nearest coordination spheres is important. This was not the case for the second-order parameters. Apparently, this is explained by the fact that the long-range electrostatic interaction, neglecting screening, is proportional to R^{-5} and R^{-7} in the case of the fourth and sixth orders, respectively, and to R^{-3} in the case of second order (R is the distance from the RE-atom to the ion).

Following the authors of the superposition model, we also assumed that in the series of experimental samples the fourth- and sixth-order crystal fields are determined by the ions in the two nearest coordination spheres: Si and Cu.

For the case of RCu_2Si_2 compounds, the equations of the superposition model for the fourth- and sixth-order crystal fields, taking account of the two coordination spheres, can be represented as follows:

$$B_l^0 = \Theta_l [\bar{K}_{l0}(\text{Si})\tilde{A}_l(\text{Si}) + \bar{K}_{l0}(\text{Cu})\tilde{A}_l(\text{Cu})],$$

$$B_l^4 = \Theta_l [\bar{K}_{l4}(\text{Si})\tilde{A}_l(\text{Si}) + \bar{K}_{l4}(\text{Cu})\tilde{A}_l(\text{Cu})], \quad l = 4, 6. \quad (6)$$

Solving the system of equations (6), we can estimate the contribution to the fourth- and sixth-order crystal fields for both ligands, silicon and copper. The values of the coordination factors \bar{K}_{lm} , calculated using the structural data from

TABLE II. Radii and coordination factors of the spheres of the ligands Si and Cu for different RE metals.

Sphere	R and \bar{K}_{lm}	Ce	Pr	Nd	Ho	Er
Si	$R, \text{\AA}$	3.136	3.130	3.115	3.040	3.024
	\bar{K}_{40}	-0.622	-0.662	-0.691	-0.818	-0.765
	\bar{K}_{44}	-25.56	-25.44	-25.35	-24.96	-25.13
	\bar{K}_{60}	2.159	2.187	2.206	2.289	2.255
	\bar{K}_{64}	-13.79	-14.23	-14.54	-15.96	-15.37
Cu	$R, \text{\AA}$	3.218	3.216	3.208	3.181	3.178
	\bar{K}_{40}	-2.467	-2.446	-2.413	-2.221	-2.194
	\bar{K}_{44}	5.761	5.708	5.630	5.206	5.150
	\bar{K}_{60}	-2.683	-2.706	-2.739	-2.910	-2.930
	\bar{K}_{64}	28.71	28.55	28.32	26.98	26.79

Ref. 15, are presented in Table II. The results for the parameters $\tilde{A}_l(\text{Si})$ and $\tilde{A}_l(\text{Cu})$ are presented in Table III, where solutions of the system of equations (6) are given for both variants of the signs of B_l^m . The variant $A_4^4 > 0$ and $A_6^4 > 0$ is designated in Table III as $(++)$ and the opposite variant is designated as $(--)$. As noted above, proceeding only from the neutron spectroscopy data for the paramagnetic state, it is impossible to determine unambiguously the sign combination for the parameters A_4^4 and A_6^4 . In Refs. 5 and 6, we presented qualitative arguments supporting the fact that the choice $A_4^4 > 0$ and $A_6^4 > 0$ is preferred. At the same time, analysis of the inelastic thermal-neutron scattering data for the magnetically ordered state, where the scattering cross section depends on the choice of the signs of A_4^4 and A_6^4 , showed that only the combination $A_4^4 > 0$ and $A_6^4 > 0$ gives acceptable agreement between the measured inelastic thermal-neutron scattering spectra at $T < T_N$ and the spectra computed in the molecular-field approximation. Therefore in what follows we shall discuss this combination of signs of the parameters A_4^4 and A_6^4 .

It can be expected that, in principle, the parameters \tilde{A}_l for the isostructural compounds RCu_2Si_2 will depend very weakly on the RE-metal ion, since they will be determined mainly by the environment of the RE-metal ion in the lattice. However, as one can see from Table III, the parameter $\tilde{A}_4(\text{Si})$ does exhibit a strong dependence on the RE-metal ion on passing from the group of compounds with Nd, Ho, and Er to compounds with Ce and Pr, while $\tilde{A}_4(\text{Cu})$ changes

TABLE III. Crystal-field parameters in the superposition model for different RE metals. The choice of signs $A_4^4 > 0$ and $A_6^4 > 0$ is designated as $++$ and the opposite variant is designated as $--$.

Parameter	Variant	Ce	Pr	Nd	Ho	Er
$\tilde{A}_4(\text{Si}), \text{meV}$	$++$	-2.58	-0.96	0.16	0.08	0.00
	$--$	2.69	1.30	0.50	0.38	0.50
$\tilde{A}_4(\text{Cu}), \text{meV}$	$++$	0.94	1.10	1.52	1.13	1.30
	$--$	-0.42	0.46	1.42	1.03	1.13
$\tilde{A}_6(\text{Si}), \text{meV}$	$++$		1.81	3.12	2.97	3.17
	$--$		0.33	-1.05	-1.76	-2.16
$\tilde{A}_6(\text{Cu}), \text{meV}$	$++$		1.14	2.19	2.22	2.34
	$--$		-0.005	-1.15	-1.50	-1.76

very little along the entire series from Er to Ce, the dominant component $A_4^4(r^4)$ for Nd, Ho, and Er being the contribution of copper ($\tilde{A}_4(\text{Cu}) \gg \tilde{A}_4(\text{Si})$). However, for the compound CeCu_2Si_2 the silicon contribution is much (2.7 times) greater than $\tilde{A}_4(\text{Cu})$ and it is negative. The situation in the case of PrCu_2Si_2 is intermediate between compounds with Ce and the compounds with Nd, Ho, and Er. For example, the absolute value of $\tilde{A}_4(\text{Si})$ is of the same order of magnitude as $\tilde{A}_4(\text{Cu})$, but it has the opposite sign. The sixth-order parameters $\tilde{A}_6(\text{Si})$ and $\tilde{A}_6(\text{Cu})$ exhibit virtually no dependence on the RE-metal ion for Nd, Ho, and Er. Their values decrease by a factor of 2 only on switching to Pr; this likewise indicates that the crystal-field parameters in the superposition model deviate substantially from their expected dependencies, which the values of \tilde{A}_6 for compounds with Nd, Ho, and Er satisfy. Therefore the comparisons presented above indicate that the values of the parameters for the compounds CeCu_2Si_2 and PrCu_2Si_2 differ substantially from the corresponding values for compounds with Nd, Ho, and Er, and on switching from the latter three compounds to the compounds with Pr and Ce the silicon contribution becomes greater than the copper contribution. The special nature of the crystal-field potential for these two compounds correlates with their anomalous electronic properties.

In the case of CeCu_2Si_2 , where the hybridization of the localized $4f$ electrons with the conduction electrons is responsible for the anomalous (heavy-fermion) properties of this compound, the most natural explanation of the differences in the crystal-field parameters from those of compounds with no such anomalies (Nd, Ho, and Er) is that the hybridization of the $4f$ electrons with the p electrons of silicon is much stronger. This interpretation was proposed in an analysis of the crystal-field parameters of CeCu_2Si_2 and NdCu_2Si_2 in our two preceding works.^{5,6} The results of the present work, which include data on the crystal field for all the compounds RCu_2Si_2 investigated, provide further confirmation of the fact that $f-p$ hybridization is responsible for the anomalous properties of the heavy-fermion system CeCu_2Si_2 . It should be noted that a recent analysis¹⁶ of the dependence of the type of ground state of the compounds CeM_2X_2 on the Ce-M and Ce-X distances also showed that their electronic properties are determined mainly by $(\text{Ce})f - (\text{X})p$ hybridization.

In a number of works¹¹⁻¹³ it has been asserted on the basis of measurements of the macroscopic properties of PrCu_2Si_2 that this compound is a heavy-fermion system because of the quadrupole scattering of the conduction electrons by the $4f$ electrons (quadrupole Kondo effect). The main experimental facts supporting this interpretation are as follows:

- the large electronic contribution to the specific heat $\gamma = 225 \text{ mJ/mole} \cdot \text{K}^2$;
- absence of anomalies in the temperature dependence of the lattice parameters, which was attributed to the compensation of the quadrupole moment of the $4f$ -electronic shell; and,
- anomalously high Néel temperature $T_N = 21 \text{ K}$.

Knowing the crystal-field parameters and, correspond-

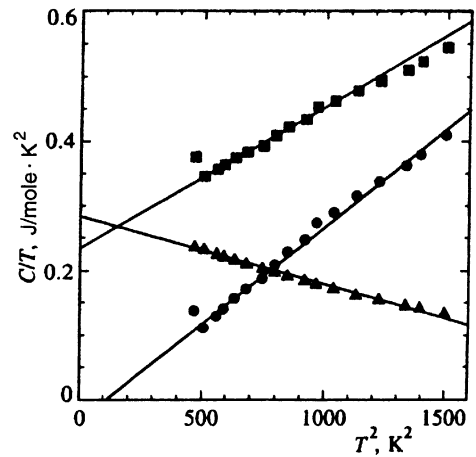


FIG. 13. Specific heat divided by T versus T^2 for PrCu_2Si_2 in the paramagnetic phase. Squares are the data of Ref. 12, triangles are the contribution to the specific heat of the Schottky anomalies computed on the basis of the crystal field parameters determined in the present work; circles are the result of subtraction from the first set. Lines are the linear extrapolations of the three sets of points.

ingly, the energy-level scheme makes it possible to show that the facts a) and b) can be interpreted as crystal-field defects. For example, the large electronic contribution to the specific heat is explained quantitatively by the Schottky anomaly, and the absence of anomalies in the temperature dependence of the lattice parameters is associated with the weak temperature dependence of the quadrupole moment of the Pr^{+3} ion in this compound. We discussed this in detail in Ref. 7. Figure 13 displays the specific heat of PrCu_2Si_2 above the Néel temperature in the coordinates C/T versus T^2 (squares) and a fit of the experimental points by a straight line, which gives the Sommerfeld constant $\gamma = 225 \text{ mJ/mole} \cdot \text{K}^2$. The figure also shows the contribution of the Schottky anomaly (triangles) to the specific heat of PrCu_2Si_2 , calculated using our set of crystal-field parameters. As one can see, the Schottky anomaly in these coordinates can be accurately approximated by a straight line, giving at the intersection of the C/T axis $\gamma = 285 \text{ mJ/mole} \cdot \text{K}^2$, which does not differ much from the value of the Sommerfeld constant. If, however, the Schottky contribution is calculated from the experimental data, then the remainder can also be described accurately by a straight line with a small negative value of γ , which to within the accuracy of extrapolations from such high temperatures agrees reasonably well with the value of the Sommerfeld constant $\gamma = 4 \text{ mJ/mole} \cdot \text{K}^2$ for the isostructural nonmagnetic analog LaCu_2Si_2 . Therefore, the high value of γ in PrCu_2Si_2 is a crystal-field effect (Schottky anomaly) and it is not associated with the anomalous electronic properties.

The interpretation of the point b) is not so unambiguous, despite the fact that it is possible to give an interpretation with the aid of the crystal field. Since the anomaly in the fourth-order crystal field of the compound PrCu_2Si_2 is very close to the anomaly exhibited by the heavy-fermion compound CeCu_2Si_2 , it is logical to conjecture that this anomaly is of the same nature: It is due to the large $f-p$ hybridization contribution to the effective potential of the crystal field. Therefore, having explained the small quadrupole moment of

the Pr^{3+} ion as a crystal-field effect, we must also answer the question of whether or not this effect is associated with the anomalous character of the crystal field.

The anomalously high value of the Néel temperature could be a strong argument in favor of the correctness of the interpretation that attributes the crystal field anomaly in the compound PrCu_2Si_2 to $f-p$ hybridization. In Ref. 12, it was shown convincingly that the RKKY exchange mechanism, which is common to all compounds in the entire series, is realized here but with an anomalously high exchange interaction constant between the $4f$ magnetic moments, which could be explained by the high value of the $f-p$ Kondo exchange integral. The situation with the compound NdCu_2Si_2 remains unclear. An estimate of the $f-f$ exchange integral in the molecular-field approximation for the three compounds RCu_2Si_2 ($R = \text{Pr, Nd, and Gd}$) gives 0.33, 0.20, and 0.22 meV, respectively. According to the de Gennes rule, the expected value for PrCu_2Si_2 should be ~ 0.01 meV. At the same time, it should be noted that the exchange integral (Néel temperature) for NdCu_2Si_2 ($T_N = 10$ K) also does not satisfy the de Gennes rule and is anomalously large. In the case of NdCu_2Si_2 , however, no anomalous behavior of the crystal field parameters is observed in the superposition model. The higher (compared with the value predicted by the de Gennes rule) Néel temperature in NdCu_2Si_2 could be due to an indirect interaction of the quadrupole moments of the Nd^{+3} ions, resulting in a deviation from the de Gennes rule. In the case of PrCu_2Si_2 , where this deviation is approximately three times larger than in NdCu_2Si_2 , such a strong discrepancy from the de Gennes rule could be due to a combination of both factors—hybridization and indirect interaction of the quadrupole moments.

6. CONCLUSIONS

A systematic investigation of the crystal field in the family of isostructural compounds RCu_2Si_2 was performed by the method of inelastic scattering of thermal neutrons. The experiments performed with two types of spectrometers at different temperatures made it possible to determine unambiguously the parameters of the phenomenological crystal-field Hamiltonian. Analysis of these parameters in the superposition model showed that the hybridization of the p

electrons of silicon with the localized f electrons of cerium makes the main contribution to the crystal-field potential in the heavy-fermion system CeCu_2Si_2 . This observation is in qualitative agreement with the theoretical estimates presented in Ref. 2. A determination of the crystal-field parameters for PrCu_2Si_2 showed that the macroscopic properties of this compound can be quantitatively interpreted as being due mainly to the splitting of the ground-state multiplet of the Pr^{+3} ion in the crystal field, though the question of the reason for the anomalously high Néel temperature in PrCu_2Si_2 and NdCu_2Si_2 remains, once again, unclear.

We are grateful to A. D. Chistyakov and N. B. Kol'chugina for preparing the samples. E. A. G. and A. Yu. M. are grateful to the Rutherford-Appleton Laboratory (Great Britain) for financial support and hospitality. This work was performed under the support of the International Science Foundation Grant No. NK4000 and US Department of Energy contract No. W-31-109-ENG-38.

¹P. Fulde and M. Loewenhaupt, *Adv. Phys.* **34**, 589 (1985).

²P. M. Levy and S. Zhang, *Phys. Rev. Lett.* **62**, 78 (1989).

³A. Szytula and J. Leciejewicz, in *Handbook on the Physics and Chemistry of Rare Earths*, edited by K. A. Gscheidner, Jr. and L. Eyring, North-Holland, Amsterdam, 1989, Vol. 12.

⁴J. A. Blanco, D. Schimitt, and J. C. Gomez Sal, *J. Magn. Magn. Mater.* **116**, 128 (1992); J. A. Blanco, D. Gignoux, and D. Schimitt, *Z. Phys. B* **89**, 343 (1992).

⁵E. A. Goremychkin and R. Osborn, *Phys. Rev. B* **47**, 14280 (1993).

⁶E. A. Goremychkin, A. Yu. Muzychka, and R. Osborn, *Physica B* **179**, 184 (1992).

⁷E. A. Goremychkin, R. Osborn, and A. Yu. Muzychka, *Phys. Rev. B* **50**, 13863 (1994).

⁸E. Holland-Moritz and D. Wohlleben, *Phys. Rev. B* **25**, 7482 (1982).

⁹K. W. H. Stevens, *Proc. Roy. Soc. A* **65**, 209 (1952).

¹⁰U. Walter, *J. Phys. Chem. Solids* **45**, 401 (1984).

¹¹E. V. Sampathkumaran, I. Das, R. Vijaraghavan *et al.*, *Sol. St. Commun.* **78**, 971 (1991).

¹²E. V. Sampathkumaran and I. Das, *J. Phys.: Cond. Matter* **4**, L475 (1992).

¹³E. V. Sampathkumaran, K. Hirota, I. Das, and M. Ishikawa, *Z. Phys. B* **90**, 195 (1993).

¹⁴D. J. Newman and B. Ng, *Rep. Progr. Phys.* **52**, 699 (1989).

¹⁵W. Schlabit, J. Baumann, G. Neumann *et al.*, in *Crystalline Electric Field Effects in f -Electron Magnetism*, edited by P. Buerlin, W. Suski, and Z. Zolnierok, Plenum Press, N. Y. (1982), p. 289.

¹⁶J. G. Sereni and O. Trovarelli, *JMM* **140-144**, 885 (1995).

Translated by M. E. Alferieff